Mean-Square Electric Dipole Moment of Oligo- and Poly(methyl methacrylate)s in Dilute Solution

Hitoshi Ando,† Takenao Yoshizaki,† Akihiro Aoki,‡ and Hiromi Yamakawa*,†

Department of Polymer Chemistry, Kyoto University, Kyoto 606-01, Japan, and Material Analysis Research Center, Teijin Limited, Hino, Tokyo 191, Japan

Received April 14, 1997; Revised Manuscript Received July 25, 1997[⊗]

ABSTRACT: The mean-square electric dipole moment $\langle\mu^2\rangle$ was determined for 12 samples of atactic (a-) oligo- and poly(methyl methacrylate)s (PMMA), each with the fraction of racemic diads $f_r = 0.79$, in the range of the weight-average degree of polymerization x_w from 3 to 1.19×10^3 and for 11 samples of isotactic (i-) PMMA and its oligomers, each with $f_r \simeq 0.01$, in the range of x_w from 3 to 5.88×10^2, both in benzene at 30.0 °C. The determination was also made for a syndiotactic (s-) PMMA sample with $f_r = 0.92$ and $x_w = 3.76 \times 10^2$ and for methyl isobutyrate in the same solvent condition. For both a- and i-PMMAs, the ratio $\langle\mu^2\rangle/x_w$ as a function of x_w decreases monotonically with increasing x_w for $x_w \lesssim 20$ and then approaches its asymptotic value $(\langle\mu^2\rangle/x_w)_\infty$, i.e., 1.92_7 and 2.12_6 D^2 for a- and i-PMMAs, respectively, indicating that the excluded-volume effect on $\langle\mu^2\rangle$ is negligibly small if any. From a comparison of these values of $(\langle\mu^2\rangle/x_w)_\infty$ along with that of $\langle\mu^2\rangle/x_w$ obtained for the s-PMMA sample, it is found that $(\langle\mu^2\rangle/x_w)_\infty$ decreases with increasing f_r. An analysis of the present experimental values for a- and i-PMMAs is made by the use of the theory for the (unperturbed) helical wormlike chain modified so as to take into account possible effects of chain ends. Then it is shown that the above dependence of $\langle\mu^2\rangle/x_w$ on x_w may be explained by this modified theory with the use of the values of the model parameters already determined from an analysis of the mean-square radius of gyration, if the local electric dipole moment vectors are properly assigned to the initiating and terminating repeat units. Unfortunately, however, any useful information about the main-chain conformations of a- and i-PMMAs cannot be obtained from an analysis of the dependence of $\langle\mu^2\rangle$ on x_w.

Introduction

In a series of recent systematic experimental studies of dilute-solution behavior of polymers in the unperturbed (Θ) state, we have been analyzing the data obtained for equilibrium conformational and steady-state transport properties on the basis of the helical wormlike (HW) chain model.[1] The polymers investigated so far are atactic polystyrene with the fraction of racemic diads $f_r = 0.59$,[2−6] atactic poly(methyl methacrylate) (a-PMMA) with $f_r = 0.79$,[7−11] and isotactic (i-) PMMA with $f_r \simeq 0.01$[12−15] as asymmetric polymers and polyisobutylene[16] and poly(dimethylsiloxane) (PDMS)[17,18] as symmetric ones. Then valuable information about the chain stiffness and local chain conformation for them has been obtained from the values of the HW model parameters determined. Among these polymers, the a-PMMA chain has been found to be of the strongest helical nature,[1] and thus a typical example of the HW chain.[7,8] On the other hand, the helical nature of the i-PMMA chain is weak. This difference is due to the difference in chain stiffness and local chain conformation which arises from that in stereochemical composition (f_r).[12] The PDMS chain has also been found to be of rather strong helical nature, although not so strong as the a-PMMA chain, from an analysis of the data for its mean-square electric dipole moment $\langle\mu^2\rangle$,[17] which shows that the ratio $\langle\mu^2\rangle/x$ as a function of the degree of polymerization x exhibits a maximum.[17,19−21] Since the a- and i-PMMA chains as well as the PDMS chain have type-B dipoles[22] perpendicular to the chain contour, it is interesting to investigate the dependence on x of $\langle\mu^2\rangle/x$ of PMMAs. This is the purpose of the present paper.

The experimental data for $\langle\mu^2\rangle$ obtained so far for PMMAs [including syndiotactic (s-) PMMA with $f_r \simeq 1.0$][23,24] are restricted to the range of rather large x where $\langle\mu^2\rangle/x$ reaches its asymptotic value in the Gaussian-chain limit and therefore are not suitable for the present analysis on the basis of the HW chain model. Recall that this requires the data in the oligomer region. The only reported result available in such a region is the one obtained by Le Févre and Sundaran[25] for methyl isobutyrate (MIB), the monomeric unit of PMMA. From a comparison of these literature data, the value of $\langle\mu^2\rangle$ of MIB (i.e., $\langle\mu^2\rangle/x$ with $x = 1$) is found to be appreciably larger than those of $\langle\mu^2\rangle/x$ for all PMMAs with sufficiently large x irrespective of the value of f_r. Thus the primary purpose of the present study is to determine experimentally the dependence on x of $\langle\mu^2\rangle/x$ of a- and i-PMMAs in the oligomer region.

Although both of the PMMA and PDMS chains have type-B (perpendicular) dipoles as mentioned above, there is a difference in the situation. The permanent local electric dipole moment vector of the latter arises from the main-chain O−Si bond, while that of the former arises from the side ester group which is not rigidly attached to the main chain. For the latter, it has been shown that valuable information about the chain stiffness and local chain conformation may be obtained from an analysis of $\langle\mu^2\rangle$ on the basis of the HW chain.[17] For the former, however, it is then not clear whether this is possible or not. The clarification of this point is the secondary purpose of the present study.

In order to compare the present results for $\langle\mu^2\rangle$ with the ones previously obtained for other static and steady-state transport properties of the PMMAs, it is desirable to carry out the present dielectric measurements in the respective Θ solvents, i.e., in acetonitrile at 44.0 and 28.0 °C for the a- and i-PMMAs, respectively, as in the previous studies.[7−15] Unfortunately, however, there

* Author to whom correspondence should be addressed.
† Kyoto University.
‡ Teijin Limited.
⊗ Abstract published in *Advance ACS Abstracts,* September 15, 1997.

S0024-9297(97)00501-9 CCC: $14.00

then arises an experimental problem. As is well-known, for a determination of $\langle\mu^2\rangle$ in dilute solution, we must use a completely or nearly nonpolar solvent, so that acetonitrile is not an appropriate solvent. Thus we have chosen benzene as a solvent. In anticipation of the analysis of results, however, we note that the excluded-volume effect on $\langle\mu^2\rangle$ of the PMMA chains having type-B dipoles may be regarded as negligibly small if any.

Experimental Section

Materials. All the a-PMMA samples used in this work are the same as those used in the previous studies of the mean-square radius of gyration $\langle S^2\rangle$ (in Θ and good solvents),[7,26] the intrinsic viscosity $[\eta]$ (in Θ and good solvents),[8,26] the mean-square optical anisotropy $\langle\Gamma^2\rangle$,[9] the scattering function P_s,[10] the translational diffusion coefficient D (in Θ and good solvents),[11,27] and the second virial coefficient A_2.[28,29] They are the fractions separated by preparative gel permeation chromatography (GPC) or fractional precipitation from the original samples prepared by group-transfer polymerization and have a fixed stereochemical composition ($f_r = 0.79$) independent of x, possessing hydrogen atoms at both ends of the chain. All the i-PMMA samples used are the same as those used in the previous studies of $\langle S^2\rangle$ (in Θ and good solvents),[12,30] $[\eta]$ (in Θ and good solvents),[14,30] $\langle\Gamma^2\rangle$,[15] P_s,[13] D,[14,27], and A_2,[31] i.e., the fractions separated by preparative GPC or fractional precipitation from the original samples prepared by living anionic polymerization or from the commercial sample 9011-14-7 from Scientific Polymer Products, Inc. They possess a *tert*-butyl group at one end of the chain and a hydrogen atom at the other except for the sample iMMc6 and have a fixed stereochemical composition ($f_r \simeq 0.01$) independent of x. The one s-PMMA sample used is the same as that used in the previous study of P_s,[32] i.e., the fraction separated by fractional precipitation from the commercial sample 28300-4 with $f_r = 0.92$ from Polymer Laboratory Ltd.

The values of the weight-average molecular weight M_w, the weight-average degree of polymerization x_w, and the ratio of M_w to the number-average molecular weight M_n for all the PMMA samples above are given in Table 1. As seen from the values of M_w/M_n, they are sufficiently narrow in molecular weight distribution for the present purpose, and, in particular, the samples OM3, OM4, iOM3, iOM4, and iOM5 are completely monodisperse.

MIB (Tokyo Kasei Kogyo Co.; 99.0% purity) was purified by distillation after dehydration by passing through a silica gel column. The solvent benzene used for the determination of $\langle\mu^2\rangle$ and the solvents cyclohexane and chlorobenzene used for the calibration of a dielectric cell were purified according to standard procedures.

Dielectric Constant. For a determination of the derivative $(d\epsilon/dw)_0$ of the dielectric constant ϵ of the solution with respect to the weight fraction w at $w = 0$, which is required for the evaluation of $\langle\mu^2\rangle$, ϵ was measured as a function of w for solutions of the PMMA samples in benzene at 30.0 °C in the frequency range from 3 to 100 KHz by the use of a transformer bridge (Ando Electric Co., Tokyo, type TR-10C) equipped with a function generator (Ando Electric Co., type WBG-9) and a null-point detector (Ando Electric Co., type BDA-9). We note that measurements were also carried out at 300 KHz and 1 MHz for the sample MM12. The dielectric cell used was a concentric cylindrical one (Ando Electric Co., type LE-22), whose sample volume and vacuum capacitance were ca. 5 cm^3 and ca. 18 pF, respectively. It was contained in a water jacket made of brass, at its temperature regulated to ±0.01 °C. The cell was calibrated at 30.0 °C using cyclohexane, benzene, and chlorobenzene as reference liquids. The used values of ϵ at 30.0 °C were 2.012 for cyclohexane, 2.263 for benzene,[33] and 5.529 for chlorobenzene. The value for cyclohexane was evaluated by interpolation from the literature values 2.020 and 2.004 at 25.0 and 35.0 °C, respectively,[33] and that for chlorobenzene from the literature values 5.670 and 5.372 at 21.0 and 40.0 °C, respectively.[33] The estimated error in the capacitance measurements is ±0.01 pF.

Table 1. Values of M_w, x_w, and M_w/M_n for Oligo- and Poly(methyl methacrylate)s

sample	M_w	x_w	M_w/M_n
a-PMMA ($f_r = 0.79$)			
OM3[a]	3.02×10^2	3	1.00
OM4	4.02×10^2	4	1.00
OM6b[b]	6.13×10^2	6.11	1.00
OM8b	8.02×10^2	8.00	1.01
OM12[c]	1.16×10^3	11.6	1.02
OM18a	1.83×10^3	18.3	1.05
OM30	2.95×10^3	29.5	1.06
OM51	5.06×10^3	50.6	1.08
OM76	7.55×10^3	75.5	1.08
MM2a	2.02×10^4	202	1.08
MM7	7.40×10^4	740	1.07
MM12	1.19×10^5	1190	1.09
i-PMMA ($f_r \simeq 0.01$)			
iOM3[d]	3.58×10^2	3	1.00
iOM4	4.58×10^2	4	1.00
iOM5	5.58×10^2	5	1.00
iOM7	7.89×10^2	7.31	1.01
iOM10[e]	1.01×10^3	9.52	1.02
iOM18	1.79×10^3	17.3	1.10
iOM31	3.12×10^3	30.6	1.04
iOM71	7.07×10^3	70.1	1.05
iMM1	1.07×10^4	106	1.05
iMM2	2.57×10^4	256	1.07
iMMc6	5.89×10^4	588	1.08
s-PMMA ($f_r = 0.92$)			
sMMc4[f]	3.76×10^4	376	1.12

[a] M_w's of OM3 and OM4 had been determined by GPC.[7] [b] M_w's of OM6b, OM8b, MM7, and MM12 had been determined from light-scattering (LS) measurements in acetonitrile at 44.0 °C.[7,29] [c] M_w's of OM12 through MM2a had been determined from LS in acetone at 25.0 °C.[7,26,28] [d] M_w's of iOM3 through iOM7 had been determined by ^{1}H NMR and GPC.[12] [e] M_w's of iOM10 through iMMc6 had been detemrined from LS in acetonitrile at 28.0 °C.[12,14] [f] M_w of sMMc4 had been determined from LS in acetonitrile at 45.0 °C.[32]

The concentrations of the test solutions were in the range from ca. 4 to 10 wt % for MIB, from ca. 4 to 8 wt % for the a-PMMA samples OM3 through OM8b, from ca. 2 to 5 wt % for the a-PMMA samples OM12 through OM76, for the i-PMMA samples iOM3 through iMM2 and for the s-PMMA sample sMMc4, and from ca. 0.5 to 3 wt % for the a-PMMA samples MM2a through MM12 and for the i-PMMA sample iMMc6. For all solutions, the observed ϵ was independent of frequency in the above range.

Refractive Index Increment. The refractive index increment $(dn/dw)_0$ as defined as the derivative of the refractive index n of the solution with respect to w at $w = 0$, which is also required for the evaluation of $\langle\mu^2\rangle$, was measured at 436 nm for all the PMMA samples in benzene at 30.0 °C by the use of a Shimadzu differential refractometer. As is well-known, $(dn/dw)_0$ is very small for PMMA in benzene, so that the concentrations of the test solutions were somewhat higher than those in the case of the usual determination of the refractive index increment in our laboratory.

Specific Volume. For a determination of the derivative $(dv/dw)_0$ of the specific volume v of the solute with respect to w at $w = 0$, which is also required for the evaluation of $\langle\mu^2\rangle$, v was determined for all the PMMA samples in benzene at 30.0 °C from the density measured with a pycnometer of the Lipkin−Davison type having the volume of 3 or 10 cm^3.

Results

Before presenting experimental results for the derivatives $(d\epsilon/dw)_0$, $(dn/dw)_0$, and $(dv/dw)_0$ of the dielectric constant ϵ, refractive index n, and specific volume v, respectively, with respect to the weight fraction w of PMMA in benzene, we briefly describe the procedure of evaluating $\langle\mu^2\rangle$ from them. It is the same as that used in the previous study of $\langle\mu^2\rangle$ of PDMS.[17]

For a dilute solution of a polar solute dissolved in a nonpolar solvent, the *molar polarization P* of the solute as defined as the polarizability of the solute molecule multiplied by $4\pi N_A/3$ with N_A the Avogadro constant may be related to $\langle\mu^2\rangle$ of the solute molecule by the Debye equation,[34]

$$P = \frac{4\pi N_A}{9k_B T}\langle\mu^2\rangle + P^D \tag{1}$$

where k_B is the Boltzmann constant, T is the absolute temperature, and P^D is the distortional polarization. As is usually done, we assume that P^D is composed of the electronic polarization P^E and the atomic one P^A as

$$P^D = P^E + P^A \tag{2}$$

Then $\langle\mu^2\rangle$ may be evaluated from the equation

$$\langle\mu^2\rangle = \frac{9k_B T}{4\pi N_A}(P - P^E - P^A) \tag{3}$$

We here adopt the Halverstadt−Kumler equations[35] for P and P^E:

$$P = \frac{\epsilon_0 - 1}{\epsilon_0 + 2}M\left[\left(\frac{dv}{dw}\right)_0 + v_0\right] + \frac{3Mv_0}{(\epsilon_0 + 2)^2}\left(\frac{d\epsilon}{dw}\right)_0 \tag{4}$$

$$P^E = \frac{n_0^2 - 1}{n_0^2 + 2}M\left[\left(\frac{dv}{dw}\right)_0 + v_0\right] + \frac{6Mn_0v_0}{(n_0^2 + 2)^2}\left(\frac{dn}{dw}\right)_0 \tag{5}$$

where the subscript 0 on the quantities ϵ, v, and n indicates the values for the pure solvent (benzene in this case). We note that in the derivation of eqs 4 and 5, the effect of the internal field has been taken into account by the use of the Clausius−Mosotti equation, and that, strictly, eq 5 has been derived by Riande and Mark[36] following the procedure of Halverstadt and Kumler. We also note that as shown by Matsuo and Stockmayer,[37] eqs 3−5 are equivalent to the equations derived by Guggenheim[38] and Smith.[39] As for P^A, any available literature values do not exist for the present case. Thus we assume that it is negligibly small compared to P^E, and simply put

$$P^A = 0 \tag{6}$$

as was usually done in earlier studies.[23,24] (We give a further discussion of this assumption in the discussion section.) Thus we evaluate $\langle\mu^2\rangle$ from eqs 3−5 with experimental values for $(d\epsilon/dw)_0$, $(dn/dw)_0$, and $(dv/dw)_0$ and with eq 6.

Now the values of $(d\epsilon/dw)_0$, $(dn/dw)_0$, and $(dv/dw)_0$ are plotted against the logarithm of x_w in Figures 1−3, respectively. In Figure 1, the values of $(d\epsilon/dw)_0(M_w/M_0x_w)$ instead of $(d\epsilon/dw)_0$ itself are plotted, where M_0 is the molecular weight of the repeat unit, since the excess dielectric constant is proportional to x_w (the number of the ester groups) but not to M_w. In these figures, the unfilled circles, triangles, and squares represent the values obtained in the present study for a-, i-, and s-PMMAs, respectively, in benzene at 30.0 °C. The two solid curves in each figure connect smoothly the data points for a-PMMA along with that for MIB and those for i-PMMA, respectively. For both polymers, it is seen that $(d\epsilon/dw)_0(M_w/M_0x_w)$ and $(dv/dw)_0$ decrease with increasing x_w for $x_w \lesssim 20$ and then approach their respective asymptotic values, while $(dn/dw)_0$ increases with increasing x_w for $x_w \lesssim 20$ and then approaches its asymptotic one. The asymptotic values of these quantities are 2.0_6, -0.33_2, and 0.003 for a-PMMA and 2.2_8, -0.34_0, and 0.008 for i-PMMA, respectively. They have been evaluated as averages of the values obtained for the four samples with the highest M_w for a-PMMA and of those for the two samples with the highest M_w for i-PMMA. The values of $(d\epsilon/dw)_0(M_w/M_0x_w)$ for i-PMMA are appreciably larger than those for a-PMMA in the range of $x_w \gtrsim 10$. The value of $(d\epsilon/dw)_0$ for the s-PMMA sample sMMc4 is somewhat smaller than its asymptotic value for a-PMMA. As for the derivatives $(dn/dw)_0$ and $(dv/dw)_0$, no appreciable dependence of them on f_r is observed.

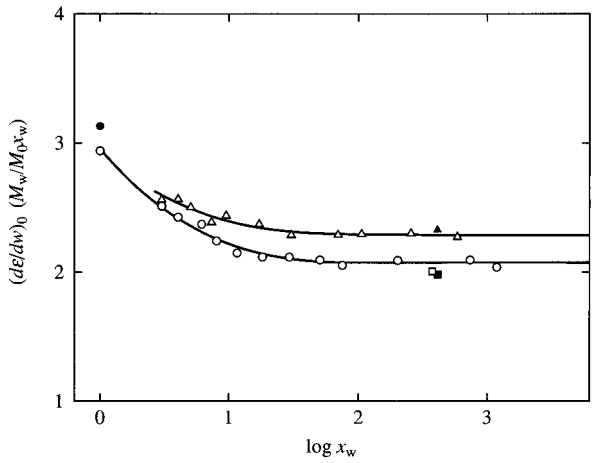

Figure 1. Plots of $(d\epsilon/dw)_0(M_w/M_0x_w)$ against the logarithm of x_w for PMMAs in benzene: (○) for a-PMMA and MIB at 30.0 °C (present data); (△) for i-PMMA at 30.0 °C (present data); (□) for s-PMMA at 30.0 °C (present data); (●) for MIB at 25.0 °C (Le Févre and Sundaran);[23] (▲) for i-PMMA at 30.0 °C (Shima et al.);[24] (■) for s-PMMA at 30.0 °C (Shima et al.).[24] The two solid curves connect smoothly the present data points for a- and i-PMMAs, respectively.

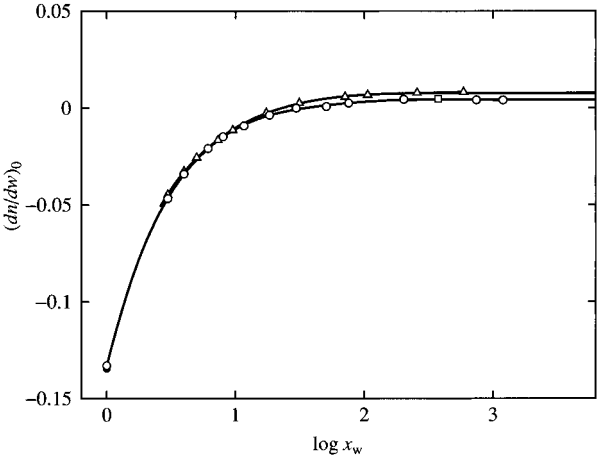

Figure 2. Plots of $(dn/dw)_0$ against the logarithm of x_w for PMMAs in benzene. The symbols have the same meaning as those in Figure 1. The two solid curves connect smoothly the present data points for a- and i-PMMAs, respectively.

In these figures are also included the values obtained by Shima et al.[24] for i-PMMA (filled triangles) and s-PMMA (filled squares) in the same solvent condition and those obtained by Le Févre and Sundaran[23] for MIB (filled circles) in benzene at 25.0 °C. The values of f_r for the i- and s-PMMA samples used by Shima et al.[24] are ca. 0.01 and 0.93, respectively, and are almost the same as those for our i- and s-PMMA samples, respec-

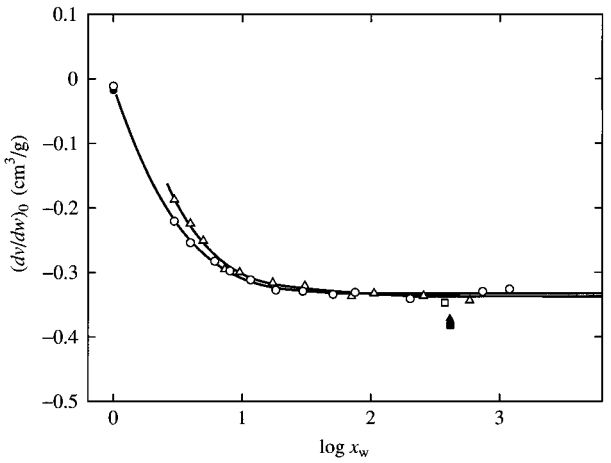

Figure 3. Plots of $(dv/dw)_0$ against the logarithm of x_w for PMMAs in benzene. The symbols have the same meaning as those in Figure 1. The two solid curves connect smoothly the present data points for a- and i-PMMAs, respectively.

tively. Thus we may directly compare the present results with theirs. Their and our values of $(d\epsilon/dw)_0 \cdot (M_w/M_0x_w)$ in Figure 1 agree well with each other for both i- and s-PMMAs, while their values of $(dv/dw)_0$ in Figure 3 are somewhat smaller than ours. We note that $(dn/dw)_0$ has not been determined by Shima et al.[24] As for MIB, the value of $(d\epsilon/dw)_0$ by Le Févre and Sundaran[23] is somewhat larger than ours, while their values of $(dn/dw)_0$ and $(dv/dw)_0$ are in good agreement with our respective values. It should be noted here that the value of ϵ observed for the a-PMMA sample MM12 is independent of the frequency of the applied electric field up to 1 MHz.

The values of P calculated from eq 4 with those of $(d\epsilon/dw)_0$ and $(dv/dw)_0$ shown in Figures 1 and 3, respectively, and the values of P^E from eq 5 with those of $(dn/dw)_0$ and $(dv/dw)_0$ shown in Figures 2 and 3, respectively, are given in Table 2. Here, the values of ϵ_0, n_0, and v_0 used for benzene at 30.0 °C are 2.263,[33] 1.516, and 1.154 cm³/g, respectively. For all the samples, the contribution of P^E is 30−40% of P. In Table 2 are also given the values of $\langle\mu^2\rangle/x_w$ calculated as mentioned above.

Discussion

Dependence of $\langle\mu^2\rangle$ on x_w. Figure 4 shows plots of the ratio $\langle\mu^2\rangle/x_w$ against the logarithm of x_w for PMMAs. The unfilled circles, triangles, and square represent the present values for a-, i-, and s-PMMAs, respectively, in benzene at 30.0 °C, and the two solid curves connect smoothly the data points for a-PMMA (including MIB) and i-PMMA, respectively. As in the case of $(d\epsilon/dw)_0$ shown in Figure 1, for both a- and i-PMMAs $\langle\mu^2\rangle/x_w$ decreases monotonically with increasing x_w for $x_w \lesssim 20$, and then approaches its asymptotic value $(\langle\mu^2\rangle/x_w)_\infty$, i.e., 1.92_7 and 2.12_6 D² for a- and i-PMMAs, respectively. These have been evaluated as averages of the values for the four samples with the highest M_w. As in the case of PDMS,[17] the excluded-volume effect on $\langle\mu^2\rangle$ for PMMAs in benzene may therefore be regarded as negligibly small if any. The data point for s-PMMA is somewhat lower than those for a-PMMA. Thus it may be concluded that $(\langle\mu^2\rangle/x_w)_\infty$ of PMMA is smaller for larger f_r.

In the figure are also shown the literature data obtained by Shima et al.[24] for i-PMMA (filled triangle) and s-PMMA (filled square) in the same solvent condition and those obtained by Le Févre and Sundaran[23] for MIB in benzene at 25.0 °C (filled circle) and by Saiz et al.[40] for MIB in carbon tetrachloride at 25 °C (right-half filled circle). All these data agree with the present ones within experimental error.

Table 2. Values of P, P^E, and $\langle\mu^2\rangle/x_w$ for Oligo- and Poly(methyl methacrylate)s in Benzene at 30.0 °C

sample	P, cm³/mol	P^E, cm³/mol	$\langle\mu^2\rangle/x_w$, D²
	a-PMMA ($f_r = 0.79$)		
MIB	$9.05_3 \times 10$	$2.74_7 \times 10$	3.13_9
OM3	$2.27_1 \times 10^2$	$7.71_4 \times 10$	2.48_7
OM4	$2.92_1 \times 10^2$	$1.01_5 \times 10^2$	2.37_2
OM6b	$4.34_3 \times 10^2$	$1.54_1 \times 10^2$	2.28_3
OM8b	$5.45_1 \times 10^2$	$2.00_7 \times 10^2$	2.14_3
OM12	$7.64_2 \times 10^2$	$2.89_2 \times 10^2$	2.03_9
OM18a	$1.18_6 \times 10^3$	$4.53_2 \times 10^2$	1.99_4
OM30	$1.91_0 \times 10^3$	$7.34_8 \times 10^2$	1.98_3
OM51	$3.24_8 \times 10^3$	$1.25_5 \times 10^3$	1.96_0
OM76	$4.79_3 \times 10^3$	$1.88_8 \times 10^3$	1.91_6
MM2a	$1.29_1 \times 10^4$	$5.01_4 \times 10^3$	1.94_6
MM7	$4.75_9 \times 10^4$	$1.86_0 \times 10^4$	1.95_0
MM12	$7.53_9 \times 10^4$	$3.00_4 \times 10^4$	1.89_7
	i-PMMA ($f_r \simeq 0.01$)		
iOM3	$2.48_9 \times 10^2$	$9.54_7 \times 10$	2.54_6
iOM4	$3.21_6 \times 10^2$	$1.20_1 \times 10^2$	2.50_8
iOM5	$3.87_7 \times 10^2$	$1.44_1 \times 10^2$	2.42_5
iOM7	$5.33_2 \times 10^2$	$1.97_3 \times 10^2$	2.28_7
iOM10	$6.97_6 \times 10^2$	$2.54_1 \times 10^2$	2.31_9
iOM18	$1.22_6 \times 10^3$	$4.50_6 \times 10^2$	2.23_0
iOM31	$2.10_4 \times 10^3$	$7.89_8 \times 10^2$	2.13_7
iOM71	$4.76_7 \times 10^3$	$1.76_8 \times 10^3$	2.12_9
iMM1	$7.23_7 \times 10^3$	$2.69_7 \times 10^3$	2.13_2
iMM2	$1.74_5 \times 10^4$	$6.46_3 \times 10^3$	2.13_5
iMMc6	$3.96_0 \times 10^4$	$1.47_0 \times 10^4$	2.10_8
	s-PMMA ($f_r = 0.92$)		
sMMc4	$2.34_3 \times 10^4$	$9.34_4 \times 10^3$	1.86_5

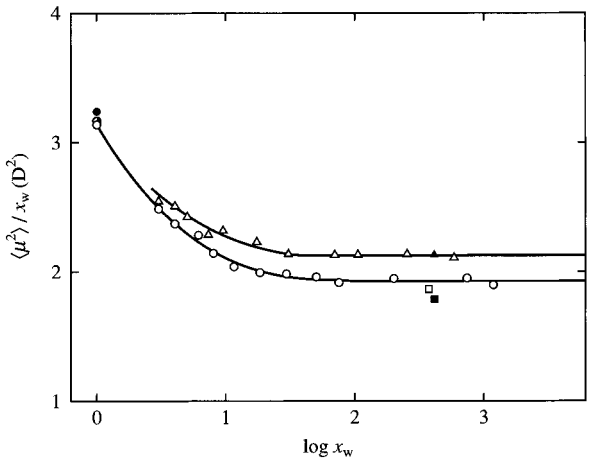

Figure 4. Plots of $\langle\mu^2\rangle/x_w$ against the logarithm of x_w for PMMAs: (○) for a-PMMA and MIB in benzene at 30.0 °C (present data); (△) for i-PMMA in benzene at 30.0 °C (present data); (□) for s-PMMA in benzene at 30.0 °C (present data); (●) for MIB in benzene at 25.0 °C (Le Févre and Sundaran);[23] (◑) for MIB in carbon tetrachloride at 25.0 °C (Saiz et al.);[40] (▲) for i-PMMA in benzene at 30.0 °C (Shima et al.);[24] (■) for s-PMMA in benzene at 30.0 °C (Shima et al.).[24] The two solid curves connect smoothly the present data points for a- and i-PMMAs, respectively.

HW Model with Effects of Chain Ends. A theoretical expression for $\langle\mu^2\rangle$ has already been derived for the HW chain having the local electric dipole moment vector uniformly affixed to a localized Cartesian coordinate system defined at every contour point.[41] As mentioned in the Introduction, the dipole moment vector of the entire PMMA chain arises mainly from the side ester groups which are not rigidly attached to the main chain. The orientations of the groups and hence of the

dipole moment vectors at the chain ends with respect to the chain contour may then be different from those in the intermediate part of the chain. Thus the above formula must be inappropriate for the PMMA chain as it stands. In this subsection, we introduce a modification to the formula in order to take into account such effects of chain ends.

Consider a *polar* HW chain of total contour length L (without excluded volume). Its equilibrium conformational behavior may be described by the constant differential geometrical curvature κ_0 and torsion τ_0 of the characteristic helix taken at the minimum of its potential energy and the static stiffness parameter λ^{-1} as defined as the bending force constant divided by $k_BT/2$. Let M_L be the shift factor as defined as the molecular weight per unit contour length of the chain and let M_0 be the molecular weight of the repeat unit, and the contour length Δs per repeat unit is given by

$$\Delta s = M_0/M_L \tag{7}$$

Assuming that the magnitudes and directions of the local electric dipole moment vectors in the repeat units at the initiating (i) and terminating (t) chain ends are different from those in the intermediate (main) units, we denote the former by $\mathbf{m}_{0,i} = (m_{\xi,i}\ m_{\eta,i},\ m_{\zeta,i})$ and $\mathbf{m}_{0,t} = (m_{\xi,t},\ m_{\eta,t},\ m_{\zeta,t})$, respectively, in the localized Cartesian coordinate systems at the contour points $\Delta s/2$ and $L - \Delta s/2$, respectively, and by $\tilde{\mathbf{m}}_{0,i}$ and $\tilde{\mathbf{m}}_{0,t}$, respectively, in an external Cartesian coordinate system. As for the intermediate ones, let $\mathbf{m}(s) = (m_\xi,\ m_\eta,\ m_\zeta)$ and $\tilde{\mathbf{m}}(s)$ be the local electric dipole moment vectors per unit length at the contour point s ($\Delta s \le s \le L - \Delta s$), expressed in the localized and external coordinate systems, respectively.

The instantaneous electric dipole moment vector $\boldsymbol{\mu}$ (in the external system) of the entire chain defined above is given by

$$\boldsymbol{\mu} = \tilde{\mathbf{m}}_{0,i} + \tilde{\mathbf{m}}_{0,t} + \int_{\Delta s}^{L-\Delta s} \tilde{\mathbf{m}}(s)\, ds \tag{8}$$

so that its mean-square electric dipole moment is given by

$$\langle \mu^2 \rangle = \langle \mu^2 \rangle_{int} + \langle \mu^2 \rangle_{end} \tag{9}$$

with

$$\langle \mu^2 \rangle_{int} = 2 \int_0^{L-2\Delta s} (L - 2\Delta s - s) \langle \tilde{\mathbf{m}}(s) \cdot \tilde{\mathbf{m}}(0) \rangle\, ds \tag{10}$$

$$\langle \mu^2 \rangle_{end} = 2 \int_{\Delta s}^{L-\Delta s} \langle \tilde{\mathbf{m}}(s) \cdot (\tilde{\mathbf{m}}_{0,i} + \tilde{\mathbf{m}}_{0,t}) \rangle\, ds + 2\langle \tilde{\mathbf{m}}_{0,i} \cdot \tilde{\mathbf{m}}_{0,t} \rangle + m_{0,i}^2 + m_{0,t}^2 \tag{11}$$

where $\langle\ \rangle$ denotes an equilibrium average and $m_{0,i}$ and $m_{0,t}$ are the magnitudes of $\mathbf{m}_{0,i}$ and $\mathbf{m}_{0,t}$, respectively.

The contribution $\langle \mu^2 \rangle_{int}$ from the intermediate (main) part of the chain is equal to $\langle \mu^2 \rangle$ of the HW chain of total contour length $L - 2\Delta s$ having the uniform local dipole moment vector $\mathbf{m}$ and may be given by[41]

$$\langle \mu^2 \rangle_{int} = (\lambda^{-1} m)^2 f_R[\lambda(L - 2\Delta s);\ \lambda^{-1}\hat{\kappa}_0,\ \lambda^{-1}\hat{\tau}_0] \tag{12}$$

with m the magnitude of $\mathbf{m}$. The function $f_R(\lambda L;\ \lambda^{-1}\kappa_0,\ \lambda^{-1}\tau_0)$ is defined from the mean-square end-to-end distance $\langle R^2 \rangle$ of the HW chain of total contour length L as

$$\langle R^2 \rangle = \lambda^{-2} f_R(\lambda L;\ \lambda^{-1}\kappa_0,\ \lambda^{-1}\tau_0) \tag{13}$$

and $\hat{\kappa}_0$ and $\hat{\tau}_0$ are defined by

$$\hat{\kappa}_0 = (\lambda^2 \nu^2 - \hat{\tau}_0^{\,2})^{1/2} \tag{14}$$

$$\hat{\tau}_0 = (\kappa_0 m_\eta + \tau_0 m_\xi)/m \tag{15}$$

where ν is given by

$$\nu = [(\lambda^{-1}\kappa_0)^2 + (\lambda^{-1}\tau_0)^2]^{1/2} = [(\lambda^{-1}\hat{\kappa}_0)^2 + (\lambda^{-1}\hat{\tau}_0)^2]^{1/2} \tag{16}$$

The function f_R is explicitly given by[42]

$$f_R(\lambda L;\ \lambda^{-1}\kappa_0,\ \lambda^{-1}\tau_0) = c_\infty \lambda L - \frac{(\lambda^{-1}\tau_0)^2}{2\nu^2} - \frac{2(\lambda^{-1}\kappa_0)^2(4 - \nu^2)}{\nu^2(4 + \nu^2)^2} + \frac{e^{-2\lambda L}}{\nu^2}\left\{\frac{(\lambda^{-1}\tau_0)^2}{2} + \frac{2(\lambda^{-1}\kappa_0)^2}{(4 + \nu^2)^2}[(4 - \nu^2)\cos(\nu\lambda L) - 4\nu \sin(\nu\lambda L)]\right\} \tag{17}$$

where

$$c_\infty = \lim_{\lambda L \to \infty} (6\lambda \langle S^2 \rangle / L) = \frac{4 + (\lambda^{-1}\tau_0)^2}{4 + \nu^2} \tag{18}$$

with $\langle S^2 \rangle$ the mean-square radius of gyration of the chain.

The additional contribution $\langle \mu^2 \rangle_{end}$ given by eq 11 may be rewritten as follows:

$$\langle \mu^2 \rangle_{end} = 2 \int_{\Delta s/2}^{L-3\Delta s/2} \langle \tilde{\mathbf{m}}_{0,i}(0) \cdot \tilde{\mathbf{m}}(s) \rangle\, ds + 2 \int_{\Delta s/2}^{L-3\Delta s/2} \langle \tilde{\mathbf{m}}(0) \cdot \tilde{\mathbf{m}}_{0,t}(s) \rangle\, ds + 2\tilde{\mathbf{m}}_{0,i}(0) \cdot \tilde{\mathbf{m}}_{0,t}(L - \Delta s) + m_{0,i}^2 + m_{0,t}^2 \tag{19}$$

where we have explicitly indicated the contour points for $\tilde{\mathbf{m}}_{0,i}$ and $\tilde{\mathbf{m}}_{0,t}$. The equilibrium averages of scalar products of the local electric dipole moment vectors and their integrals may be straightforwardly evaluated by the same method as that in the calculation of $\langle \mu^2 \rangle_{int}$,[41] i.e., first expressing the scalar products in terms of the products of the spherical vector components of the dipole moment vectors and then rewriting the latter products in terms of the angular correlation functions.[43] For simplicity, we give explicitly only the results required for the evaluation of $\langle \mu^2 \rangle_{end}$. For example, the equilibrium average of the scalar product of $\tilde{\mathbf{m}}_{0,i}$ and $\tilde{\mathbf{m}}_{0,t}$ is given by

$$\langle \tilde{\mathbf{m}}_{0,i}(0) \cdot \tilde{\mathbf{m}}_{0,t}(L) \rangle = e^{-2\lambda L}\left\{\frac{m_{0,i} m_{0,t} (\lambda^{-1}\hat{\tau}_{0,i})(\lambda^{-1}\hat{\tau}_{0,t})}{\nu^2} + \left[\mathbf{m}_{0,i} \cdot \mathbf{m}_{0,t} - \frac{m_{0,i} m_{0,t} (\lambda^{-1}\hat{\tau}_{0,i})(\lambda^{-1}\hat{\tau}_{0,t})}{\nu^2}\right]\cos(\nu\lambda L) - \left[\frac{\lambda^{-1}\kappa_0}{\nu}(m_{\zeta,i} m_{\xi,t} - m_{\xi,i} m_{\zeta,t}) + \frac{\lambda^{-1}\tau_0}{\nu}(m_{\xi,i} m_{\eta,t} - m_{\eta,i} m_{\xi,t})\right]\sin(\nu\lambda L)\right\} \tag{20}$$

Integrating this result with $\mathbf{m}$ in place of $\tilde{\mathbf{m}}_{0,t}$ over L, we obtain

$$\int_0^L \langle \tilde{\mathbf{m}}_{0,i}(0)\cdot\tilde{\mathbf{m}}(s)\rangle \, ds = \frac{(\lambda^{-1}m)m_{0,i}(\lambda^{-1}\hat{\tau}_0)(\lambda^{-1}\hat{\tau}_{0,i})}{2\nu^2} \times (1 - e^{-2\lambda L}) + \frac{1}{4+\nu^2}\left[(\lambda^{-1}\mathbf{m})\cdot\mathbf{m}_{0,i} - \frac{(\lambda^{-1}m)m_{0,i}(\lambda^{-1}\hat{\tau}_0)(\lambda^{-1}\hat{\tau}_{0,i})}{\nu^2}\right] \times \{2 - e^{-2\lambda L}[2\cos(\nu\lambda L) - \nu\sin(\nu\lambda L)]\} - \frac{1}{4+\nu^2}\left\{\frac{\lambda^{-1}\kappa_0}{\nu}[m_{\zeta,i}(\lambda^{-1}m_\xi) - m_{\xi,i}(\lambda^{-1}m_\zeta)] + \frac{\lambda^{-1}\tau_0}{\nu}[m_{\xi,i}(\lambda^{-1}m_\eta) - m_{\eta,i}(\lambda^{-1}m_\xi)]\right\}\{\nu - e^{-2\lambda L}[\nu\cos(\nu\lambda L) + 2\sin(\nu\lambda L)]\} \quad (21)$$

By the use of this equation, we may evaluate the first integral on the right-hand side of eq 19 as the difference between the integrals from 0 to $L - 3\Delta s/2$ and from 0 to $\Delta s/2$. The similar integral of $\langle \tilde{\mathbf{m}}(0)\cdot\tilde{\mathbf{m}}_{0,t}(s)\rangle$, which is required for the evaluation of the second integral on the right-hand side of eq 19, may be given by the right-hand side of eq 21 with $\lambda^{-1}\mathbf{m}$ and $\mathbf{m}_{0,t}$ in place of $\mathbf{m}_{0,i}$ and $\lambda^{-1}\mathbf{m}$, respectively.

The desired expression for $\langle\mu^2\rangle$ for the HW chain with the effects of chain ends is given by eq 9 with eqs 12, 17, 19, 20, and 21.

Local Electric Dipole Moment Vectors. As pointed out by Vacatello and Flory[44] and by Sundararajan[45] in their determination of the statistical weight matrices of the rotational isomeric state (RIS) model[46] for PMMA, the orientation of the side ester group with respect to the PMMA chain backbone is not independent of the main-chain conformation. Because of this fact, the assignment of the local electric dipole moment vector $\mathbf{m}$ (along with $\mathbf{m}_{0,i}$ and $\mathbf{m}_{0,t}$) to the HW chain for PMMA is rather complicated compared to the case of the PDMS chain[17] (for which $\mathbf{m}_{0,i}$ and $\mathbf{m}_{0,t}$ are not necessary to introduce). For the i- and a-PMMA chains, we estimate $\mathbf{m}$ on the basis of their preferred conformations generated by CONFLEX.[47] As for $\mathbf{m}_{0,i}$ and $\mathbf{m}_{0,t}$, we determine them in the next subsection so that the HW theoretical values of $\langle\mu^2\rangle$ agree well with the experimental ones.

In order to evaluate the components m_ξ, m_η, and m_ζ of $\mathbf{m}$, it is necessary to affix a localized Cartesian coordinate system (ξ, η, ζ) to a certain rigid body part composed of two successive main-chain C−C bonds corresponding to that of the HW chain.[43] There are two choices for such two successive bonds, i.e., (i) C−C$^\alpha$ (α carbon) and C$^\alpha$−C and (ii) C$^\alpha$−C and C−C$^\alpha$.[43] In each case, the manner in which the localized coordinate system is affixed to the rigid body part was established on the basis of an analysis of the RIS data for the real part of the angular correlation function of rank 1, and it was shown that there is no essential difference between the types (i) and (ii). In the present case, it is convenient to adopt the type (ii) for the following reason. If the *permanent* local electric dipole moment vectors associated with two successive repeat units of a given polymer chain prefer to be antiparallel to each other, then they cancel out with each other, and therefore the magnitude of a resultant *effective* local electric dipole moment vector per repeat unit becomes much smaller than that of the permanent one. Thus it is pertinent to take account of the contributions of two successive ester groups at the same time. It should be noted here that we simply adopted the type (i) in the previous studies of $\langle\Gamma^2\rangle$ of a-PMMA[9] and i-PMMA[15], where the relevant local quantity is not a vector but a tensor, i.e., the local polarizability tensor. The diagonal elements of such a tensor quantity are invariant to a rotation of 180° around an arbitrary axis, so that it does not suffer the cancellation such as mentioned above for the vector.

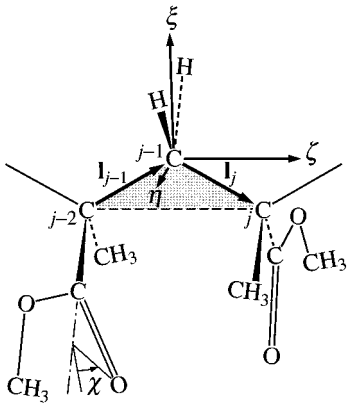

Figure 5. Rigid body part composed of the successive $C^\alpha_{j-2} - C_{j-1}$ and $C_{j-1} - C^\alpha_j$ bonds of the PMMA chain and the localized coordinate system affixed to it (see the text).

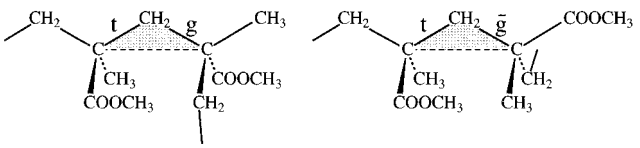

Figure 6. Preferred conformations of the i-PMMA chain: (a) *tg* conformation and (b) *tḡ* conformation (see the text).

For illustration, a rigid body part and the localized coordinate system associated with it are shown in Figure 5. The shaded triangle represents the rigid body part composed of the two successive $C^\alpha_{j-2} - C_{j-1}$ and $C_{j-1} - C^\alpha_j$ bonds (or the bond vectors $\mathbf{l}_{j-1}$ and $\mathbf{l}_j$). The ζ axis of the localized system is parallel to the vector $\mathbf{l}_{j-1} + \mathbf{l}_j$, the ξ axis is in the plane of $\mathbf{l}_{j-1}$ and $\mathbf{l}_j$, and the η axis completes the right-handed system. As also shown in the figure, we specify the orientation of the side ester group with respect to the rigid body part by a rotation angle χ around the bond vector from C$^\alpha$ to the carbonyl carbon atom, taking $\chi = 0$ if the three successive bonds CH$_3$−C$^\alpha$−C=O is in the *cis* conformation.

In order to investigate preferred conformations of PMMA chains, conformations of the heptamer ($x = 7$) of i- and s-PMMAs have been generated by CONFLEX with the MM2(77) force field and parameters[48] and with the literature values of bond dipoles.[49] For each polymer, 2048 conformations with the lowest total conformational energies have been sampled, and then ten and odd samples with the lowest, nearly equal energies of them have been investigated. Then it is found for the intermediate part of the i-PMMA heptamer that the rotational states associated with two successive main-chain bonds C$^\alpha$−C and C−C$^\alpha$ prefer to be in the states *tg* and *tḡ* (and also *gt* and *ḡt*), where *t*, *g*, and *ḡ* indicate the *trans*, *gauche*, and other *gauche* states, respectively, in the new Flory convention.[50] We note that although *t*, *g*, and *ḡ* in the CONFLEX results do not exactly correspond to the rotation angles of 0°, 120°, and −120°, respectively, but to their respective vicinities, these values are used as the rotation angles in the following analysis, for simplicity. In Figure 6 are schematically depicted the two preferred conformations of the i-PMMA chain: (a) *tg* conformation and (b) *tḡ* conformation. It is also found that in both cases χ takes ca. 0° and 180°

for the left ester group, and ca. −60° and 120° for the right one. As for the intermediate part of the s-PMMA heptamer, the *tt* conformation is found to be preferred. (This is consistent with the well-known result for the RIS model.[51]) For this conformation of the s-PMMA chain, χ takes ca. 0° and 180° for both ester groups. We note that preferred conformations of this kind were also investigated by Suter et al.[52] for polyisobutylene and by Vacatello and Flory[44] for PMMA in a different way.

On the basis of the above CONFLEX results, we estimate the local electric dipole moment vector $\mathbf{m}_0$ per rigid body part as follows. For the i-PMMA chain, we may simply assume that the above preferred conformations of the rigid body part with the two ester groups, the number of which is eight, have the same energy and hence statistical weight and therefore adopt as $\mathbf{m}_0$ an average of the dipole moment vectors for them. We then have

$$\mathbf{m}_0 = (0.5_6, -0.2_7, 0)\ \mathrm{D} \qquad \text{(i-PMMA)} \qquad (22)$$

In this evaluation, we have used the following values of the bond angles: 110.0° for C−C$^\alpha$−C, 109.5° for C−C$^\alpha$−C*, 122.0° for C$^\alpha$−C−C$^\alpha$, 114.0° for C$^\alpha$−C*−O, 121.0° for C$^\alpha$−C*═O, 113.0° for C*−O−C, and 109.5° for H−C−H, with C* indicating the carbonyl carbon.[51] We have also used the value 0.4 D of the C−H bond dipole moment,[49] the value 1.5_2 D of the ester-group dipole moment, and the value 123° of the angle between the vector C → C* and the ester-group dipole moment vector estimated by Saiz et al.[40] (The angle 123° corresponds to the fact that the group dipole moment vector is nearly parallel to the O ⇒ C bond vector.) The group dipole moment has been determined from the present experimental value 3.13_9 D^2 of $\langle\mu^2\rangle$ for MIB with the above values of the C−H bond dipole moment and the angle. For the s-PMMA chain, we similarly obtain

$$\mathbf{m}_0 = (0.7_1, 0, 0)\ \mathrm{D} \qquad \text{(s-PMMA)} \qquad (23)$$

As for a-PMMA ($f_r = 0.79$), we regard it as a random copolymer of i- and s-PMMAs to assume that $\mathbf{m}_0$ is given by

$$\begin{aligned}\mathbf{m}_0 &= (1 - f_r)\mathbf{m}_{0,\text{i-PMMA}} + f_r\mathbf{m}_{0,\text{s-PMMA}} \\ &= (0.6_8, -0.0_6, 0)\ \mathrm{D} \qquad \text{(a-PMMA)}\end{aligned} \qquad (24)$$

The local electric dipole moment vector $\mathbf{m}$ per unit contour length is related to $\mathbf{m}_0$ by the equation,

$$\mathbf{m} = (M_L/M_0)\mathbf{m}_0 \qquad (25)$$

Note that $M_0 = 100$ for PMMAs.

Finally, we examine the behavior of the HW theoretical values of $\langle\mu^2\rangle$ using the values of $\mathbf{m}$ (or $\mathbf{m}_0$) determined above. For the end dipole moment vectors $\mathbf{m}_{0,i}$ and $\mathbf{m}_{0,t}$, we consider three cases: (1) $\mathbf{m}_{0,i} = \mathbf{m}_{0,t} =$ (1.77, 0, 0) D; (2) $\mathbf{m}_{0,i} = \mathbf{m}_{0,t} =$ (0, 1.77, 0) D; (3) $\mathbf{m}_{0,i} = -\mathbf{m}_{0,t} =$ (0, 0, 1.77) D, for convenience. We note that the value 1.77 D corresponds to the observed dipole moment of MIB ($\sqrt{3.13_9}$). Figure 7 shows plots of $\langle\mu^2\rangle/x$ against the logarithm of x. The solid, dashed, and dotted curves represent the values of $\langle\mu^2\rangle/x$, $\langle\mu^2\rangle_{int}/x$, and $\langle\mu^2\rangle_{end}/x$ calculated from eqs 9, 12, and 19, respectively, with the values of $\mathbf{m}$ given by eq 25 with eqs 22 and 24. The heavy and light curves represent the values for a- and i-PMMAs, respectively, and the numbers attached to the curves indicate the cases of $\mathbf{m}_{0,i}$ and $\mathbf{m}_{0,t}$. In the calculation, we have used the values of the HW model parameters: $\lambda^{-1}\kappa_0 = 4.0$, $\lambda^{-1}\tau_0 = 1.1$, $\lambda^{-1} = 57.9$ Å, and $M_L = 36.3$ Å^{-1} for a-PMMA[7] and $\lambda^{-1}\kappa_0 = 2.5$, $\lambda^{-1}\tau_0 = 1.3$, $\lambda^{-1} = 38.0$ Å, and $M_L = 32.5$ Å^{-1} for i-PMMA,[12] which were determined from an analysis of the dependence of $\langle S^2\rangle/x_w$ on x_w. It is seen that $\langle\mu^2\rangle_{end}/x$ almost vanishes for $x \gtrsim 300$ in all cases, and therefore $\langle\mu^2\rangle/x$ becomes identical with $\langle\mu^2\rangle_{int}/x$ in this range of x. The theoretical (asymptotic) values of $(\langle\mu^2\rangle/x)_\infty$ are 1.9_0 and 2.0_7 D^2 for a- and i-PMMAs, respectively, and are in rather good agreement with the respective experimental values (1.92_7 and 2.12_6 for a- and i-PMMAs, respectively), indicating that the above estimates of $\mathbf{m}$ are reasonable. It is also seen that in the range of $x \lesssim 100$ (oligomer region) the behavior of $\langle\mu^2\rangle/x$ depends remarkably on $\mathbf{m}_{0,i}$ and $\mathbf{m}_{0,t}$ through $\langle\mu^2\rangle_{end}/x$. As in the cases of $\langle R^2\rangle$ and $\langle S^2\rangle$,[1] $\langle\mu^2\rangle_{int}/x$ for a-PMMA as a function of x exhibits a maximum. It is interesting to note that the behavior of $\langle\mu^2\rangle_{end}/x$ depends on the HW model parameters as well as that of $\langle\mu^2\rangle_{int}/x$.

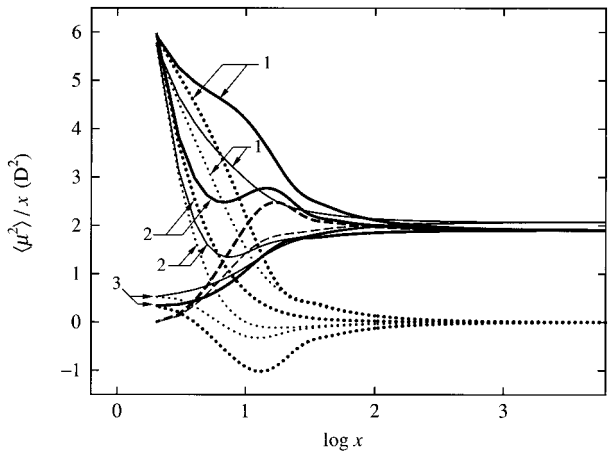

Figure 7. Plots of $\langle\mu^2\rangle/x$ against the logarithm of x. The heavy and light curves represent the HW theoretical values for a- and i-PMMAs, respectively. The solid, dashed, and dotted curves represent the values of $\langle\mu^2\rangle/x$, $\langle\mu^2\rangle_{int}/x$, and $\langle\mu^2\rangle_{end}/x$, respectively. The numbers attached to the curves indicate three cases of the end dipole moment vectors: (1) $\mathbf{m}_{0,i} = \mathbf{m}_{0,t}$ = (1.77, 0, 0) D; (2) $\mathbf{m}_{0,i} = \mathbf{m}_{0,t}$ = (0, 1.77, 0) D; (3) $\mathbf{m}_{0,i} = -\mathbf{m}_{0,t}$ = (0, 0, 1.77) D.

Comparison with the HW Theory. Figure 8 shows plots of $\langle\mu^2\rangle/x_w$ against the logarithm of x_w. The circles and triangles represent the present experimental values for a- and i-PMMAs, respectively, in benzene at 30.0 °C. The heavy and light solid curves represent the respective best-fit HW theoretical values calculated from eq 9 with eqs 12 and 19 with the values of the HW model parameters given in the last subsection. We have used the values (0.6_5, -0.1_1, 0) and (0.5_7, -0.2_7, 0) of $\mathbf{m}$ for a- and i-PMMAs, respectively, which are not exactly the same as those estimated in the last subsection, but which have been somewhat modified so that the theoretical asymptotic values $(\langle\mu^2\rangle/x_w)_\infty$ become identical with the respective observed values. As already mentioned, the values of $\mathbf{m}_{0,i}$ and $\mathbf{m}_{0,t}$ have been chosen so that the theoretical values in the oligomer region are in good agreement with the experimental ones, and we have used $\mathbf{m}_{0,i} = (1.3, 0, 1.7)$ D and $\mathbf{m}_{0,t} = (1.3, 0, -1.7)$ D for a-PMMA and $\mathbf{m}_{0,i} = (1.2, -0.55, 1.1)$ D and $\mathbf{m}_{0,t} = (1.2, -0.55, -1.1)$ D for i-PMMA. From these values of $\mathbf{m}_{0,i}$ and $\mathbf{m}_{0,t}$, we have $m_{0,i} = m_{0,t} = 2.1_4$ D for a-PMMA and $m_{0,i} = m_{0,t} = 1.7_2$ D for i-PMMA, which are not very different from the value 1.77 D of the dipole moment of MIB. It is interesting to point out that the ζ components of $\mathbf{m}_{0,i}$ and $\mathbf{m}_{0,t}$ have opposite signs for both PMMAs.

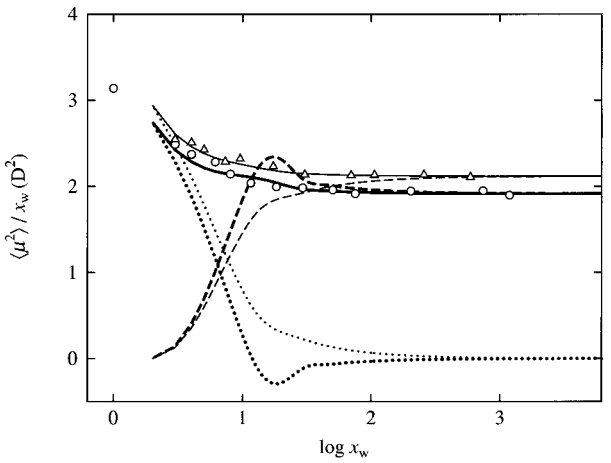

Figure 8. Plots of $\langle\mu^2\rangle/x_w$ against the logarithm of x_w. The circles and triangles represent the present experimental values for a- and i-PMMAs, respectively, in benzene at 30.0 °C. The heavy and light solid curves represent the respective best-fit HW theoretical values. The dashed and dotted curves represent the theoretical values of $\langle\mu^2\rangle_{int}/x$ and $\langle\mu^2\rangle_{end}/x$, respectively, with their thickness having the same meaning as above.

In the Experimental Section, we have assumed the vanishing atomic polarization P^A in the experimental evaluation of $\langle\mu^2\rangle$, as usually done for almost all polymers except for PDMS.[53] Considering the previous experimental determination of $\langle\mu^2\rangle$ of PDMS,[17] for which P^A cannot be neglected, its effect must be remarkably large in the oligomer region if it exists. Thus the above reasonable values of $m_{0,i}$ and $m_{0,t}$ indicate that P^A of PMMA is negligibly small if any.

In the figure, the dashed and dotted curves represent the theoretical values of $\langle\mu^2\rangle_{int}/x$ and $\langle\mu^2\rangle_{end}/x$ calculated from eqs 12 and 19, respectively, with the above-mentioned parameter values, the heavy and light curves representing the values for a- and i-PMMAs, respectively. It is seen for the HW theoretical values for a-PMMA that the maximum in $\langle\mu^2\rangle_{int}/x$ is canceled out by the minimum in $\langle\mu^2\rangle_{end}/x$, and then the resultant $\langle\mu^2\rangle/x$ becomes a monotonically decreasing function of x, although there still remain small inflections. For both a- and i-PMMAs, the behavior of $\langle\mu^2\rangle/x_w$ as a function of x_w in the oligomer region may be regarded as arising from $\langle\mu^2\rangle_{end}/x_w$, indicating that information about the main-chain conformations of a- and i-PMMAs cannot be obtained from an analysis of the dependence of $\langle\mu^2\rangle/x_w$ on x_w, in contrast to the case of PDMS.[17]

The present modification of the HW theory of $\langle\mu^2\rangle$ is a zeroth-order approximation. We may further pursue this line by taking account of the effects of the dipole moment vectors in the neighborhood of the chain ends. Then, however, we must consider also the correlation between the main-chain conformation and the side-group orientation, and the analytical evaluation is difficult to carry out. Note also that a computer simulation like CONFLEX is restricted to the oligomer region for very small x.

Conclusion

We have determined $\langle\mu^2\rangle$ for a-PMMA with $f_r = 0.79$ and for i-PMMA with $f_r \simeq 0.01$ in benzene at 30.0 °C over a wide range of the weight-average degree of polymerization x_w, including the oligomer region. The determination has also been made for an s-PMMA sample with $f_r = 0.92$ and with sufficiently large x_w. For both a- and i-PMMAs, $\langle\mu^2\rangle/x_w$ as a function of x_w decreases monotonically with increasing x_w for $x_w \lesssim 20$ and then approaches its asymptotic value $(\langle\mu^2\rangle/x_w)_\infty$, indicating that the excluded-volume effect on $\langle\mu^2\rangle$ is negligibly small if any. From a comparison of these values of $(\langle\mu^2\rangle/x_w)_\infty$ along with that of $\langle\mu^2\rangle/x_w$ obtained for the s-PMMA sample, it is found that $(\langle\mu^2\rangle/x_w)_\infty$ decreases with increasing f_r. The above dependence of $\langle\mu^2\rangle/x_w$ on x_w may be explained by the HW theory[41] with the use of the values of the model parameters already determined from an analysis of the dependence $\langle S^2\rangle/x_w$ on x_w,[7,12] if the effects of chain ends are appropriately taken into account. Unfortunately, however, it is then clear that any useful information about the main-chain conformations of a- and i-PMMAs cannot be obtained (or the HW model parameters cannot be determined) from an analysis of the dependence of $\langle\mu^2\rangle/x_w$ on x_w. This arises from the fact that there is a correlation between the conformation of the main chain and the orientation of the side ester group, the latter being the main source of $\langle\mu^2\rangle$ of PMMA. This is in contrast to the case of PDMS having *rigid* type-B dipoles.

References and Notes

(1) Yamakawa, H. *Helical Wormlike Chains in Polymer Solutions*; Springer: Berlin, 1997.
(2) Konishi, T.; Yoshizaki, T.; Shimada, J.; Yamakawa, H. *Macromolecules* **1989**, *22*, 1921.
(3) Einaga, Y.; Koyama, H.; Konishi, T.; Yamakawa, H. *Macromolecules* **1989**, *22*, 3149.
(4) Konishi, T.; Yoshizaki, T.; Saito, T.; Einaga, Y.; Yamakawa, H. *Macromolecules* **1990**, *23*, 290.
(5) Koyama, H.; Yoshizaki, T.; Einaga, Y.; Hayashi, H.; Yamakawa, H. *Macromolecules* **1991**, *24*, 932.
(6) Yamada, T.; Yoshizaki, T.; Yamakawa, H. *Macromolecules* **1992**, *25*, 377.
(7) Tamai, Y.; Konishi, T.; Einaga, Y.; Fujii, M.; Yamakawa, H. *Macromolecules* **1990**, *23*, 4067.
(8) Fujii, Y.; Tamai, Y.; Konishi, T.; Yamakawa, H. *Macromolecules* **1991**, *24*, 1608.
(9) Takaeda, Y.; Yoshizaki, T.; Yamakawa, H. *Macromolecules* **1993**, *26*, 3742.
(10) Yoshizaki, T.; Hayashi, H.; Yamakawa, H. *Macromolecules* **1993**, *26*, 4037.
(11) Dehara, K.; Yoshizaki, T.; Yamakawa, H. *Macromolecules* **1993**, *26*, 5137.
(12) Kamijo, M.; Sawatari, N.; Konishi, T.; Yoshizaki, T.; Yamakawa, H. *Macromolecules* **1994**, *27*, 5697.
(13) Horita, K.; Yoshizaki, T.; Hayashi, H.; Yamakawa, H. *Macromolecules* **1994**, *27*, 6492.
(14) Sawatari, N.; Konishi, T.; Yoshizaki, T.; Yamakawa, H. *Macromolecules* **1995**, *28*, 1089.
(15) Naito, Y.; Sawatari, N.; Takaeda, Y.; Yoshizaki, T.; Yamakawa, H. *Macromolecules* **1997**, *30*, 2751.
(16) Abe, F.; Einaga, Y.; Yamakawa, H. *Macromolecules* **1991**, *24*, 4423.
(17) Yamada, T.; Yoshizaki, T.; Yamakawa, H. *Macromolecules* **1992**, *25*, 1487.
(18) Yamada, T.; Koyama, H.; Yoshizaki, T.; Einaga, Y.; Yamakawa, H. *Macromolecules* **1993**, *26*, 2566.
(19) Sutton, C.; Mark, J. E. *J. Chem. Phys.* **1971**, *54*, 5011.
(20) Liao, S. C.; Mark, J. E. *J. Chem. Phys.* **1973**, *59*, 3825.
(21) Beevers, M. S.; Mumby, S. J.; Clarson, S. J.; Semlyen, J. A. *Polymer* **1983**, *24*, 1565.
(22) Stockmayer, W. H. *Pure Appl. Chem.* **1967**, *15*, 539.
(23) Le Févre, R. J. W.; Sundaran, K. M. S. *J. Chem. Soc.* **1963**, 1880.
(24) Shima, M.; Sato, M.; Atsumi, M.; Hatada, K. *Polym. J.* **1994**, *26*, 579 and references cited therein.
(25) Le Févre, R. J. W.; Sundaran, A. *J. Chem. Soc.* **1962**, 3904.
(26) Abe, F.; Horita, K.; Einaga, Y.; Yamakawa, H. *Macromolecules* **1994**, *27*, 725.
(27) Arai, T.; Sawatari, N.; Yoshizaki, T.; Einaga, Y.; Yamakawa, H. *Macromolecules* **1996**, *29*, 2309.
(28) Abe, F.; Einaga, Y.; Yamakawa, H. *Macromolecules* **1994**, *27*, 3262.
(29) Abe, F.; Einaga, Y.; Yamakawa, H. *Macromolecules* **1995**, *28*, 695.
(30) Kamijo, M.; Abe, F.; Einaga, Y.; Yamakawa, H. *Macromolecules* **1995**, *28*, 1095.

(31) Kamijo, M.; Abe, F.; Einaga, Y.; Yamakawa, H. *Macromolecules* **1995**, *28*, 4159.
(32) Yoshizaki, T.; Hayashi, H.; Yamakawa, H. *Macromolecules* **1994**, *27*, 4259.
(33) Le Févre, R. J. W. *Trans. Faraday Soc.* **1938**, *34*, 1127.
(34) Debye, P. *Polar Molecules*; Chemical Catalog: New York, 1929.
(35) Halverstadt, L. F.; Kumler, W. D. *J. Am. Chem. Soc.* **1942**, *64*, 2988.
(36) Riande, E.; Mark, J. E. *Eur. Polym. J.* **1984**, *20*, 517.
(37) Matsuo, K.; Stockmayer, W. H. *J. Phys. Chem.* **1981**, *85*, 3307.
(38) Guggenheim, E. A. *Trans. Faraday Soc.* **1949**, *45*, 714.
(39) Smith, J. W. *Electric Dipole Moments*; Butterworths: London, 1955; p 47.
(40) Saiz, E.; Hummel, J. P.; Flory, P. J.; Plavšić, M. *J. Phys. Chem.* **1981**, *85*, 3211.
(41) Yamakawa, H.; Shimada, J.; Nagasaka, K. *J. Chem. Phys.* **1979**, *71*, 3573; see also chapter 5 of ref 1.
(42) Yamakawa, H.; Fujii, M. *J. Chem. Phys.* **1976**, *64*, 5222; see also chapter 4 of ref 1.
(43) Yamakawa, H.; Shimada, J. *J. Chem. Phys.* **1979**, *70*, 609; see also chapter 4 of ref 1.
(44) Vacatello, M.; Flory, P. J. *Macromolecules* **1986**, *19*, 405.
(45) Sundararajan, P. R. *Macromolecules* **1986**, *19*, 415.
(46) Flory, P. J. *Statistical Mechanics of Chain Molecules*; Interscience: New York, 1969.
(47) Goto, H.; Osawa, E. *J. Am. Chem. Soc.* **1989**, *111*, 8950.
(48) Allinger, N. L. *J. Am. Chem. Soc.* **1977**, *99*, 8127.
(49) Smyth, C. P. *Dielectric Behavior and Structure*; McGraw-Hill: New York, 1955.
(50) Flory, P. J.; Sundararajan, P. R.; DeBolt, L. C. *J. Am. Chem. Soc.* **1974**, *96*, 5015.
(51) Sundararajan, P. R.; Flory, P. J. *J. Am. Chem. Soc.* **1974**, *96*, 5025.
(52) Suter, U. W.; Saiz, E.; Flory, P. J. *Macromolecules* **1983**, *16*, 1317.
(53) Riande, E.; Saiz, E. *Dipole Moments and Birefringence of Polymers*; Prentice Hall: Englewood Cliffs, N.J., 1992.

MA970501D